ISSN 1087-6596, Glass Physics and Chemistry, 2020, Vol. 46, No. 4, pp. 321–328. © Pleiades Publishing, Ltd., 2020.
Russian Text © The Author(s), 2020, published in Fizika i Khimiya Stekla.

Stability of a Two-Layer Silicene on a Nickel Substrate upon Intercalation of Graphite

A. E. Galashev[a, b] and O. R. Rakhmanova[a, b, *]

[a] *Institute of High-Temperature Electrochemistry, Ural Branch, Russian Academy of Sciences, Yekaterinburg, 620990 Russia*
[b] *Ural Federal University, Yekaterinburg, 620002 Russia*
**e-mail: oksana_rahmanova@mail.ru*

Received May 30, 2019; revised February 4, 2020; accepted April 3, 2020

Abstract—The processes of lithization and delithization of a perfect and defective (containing monovacancies) silicene channel located on an Ni(111) substrate are studied in a molecular-dynamic (MD) experiment. It is shown that such a system can exist up to 1 ns in time without destruction. The limiting amount of lithium ions intercalated into the silicene channel modified by monovacancies is 20% higher than for a defect-free structure. At the same time, the silicene sheets are not destroyed and retain their integrity. The predominant observed arrangement of lithium atoms in the channel is above the centers of the hexagonal silicon rings. In the channel formed by perfect silicene, the lithium mobility coefficient is twice as high as in a defective structure. In general, nickel as a substrate for a silicene channel can be a promising material in terms of achieving high dynamic capacity of a silicene electrode for lithium-ion batteries.

Keywords: intercalation/deintercalation, diffusion coefficients, lithium, monovacancies, molecular dynamics, nickel, substrate, silicene

DOI: 10.1134/S1087659620040069

INTRODUCTION

Currently, there is a need to develop materials for efficient and stable anodes suitable for next-generation high-performance lithium-ion batteries (LIBs). Two-dimensional materials are considered as promising for such LIBs. In addition to the widely studied 2D structures, such as graphene and silicene, borofen (β_1^s), for which the theoretical expected charge capacity is quadruple that of graphene and the expected charge/discharge rate is 2–3 orders of magnitude higher than that of a similar silicene electrode, has also attracted the attention of researchers [1]. However, this 2D material has been studied only theoretically and has not been prepared experimentally. In addition to LIBs, the possibility of creating sodium-ion batteries (SIBs) is being considered [2]. The quantum-mechanical calculations of the interaction of Na and silicene in the context of the creation of SIBs indicate the possibility of adsorption of sodium ions on silicene sheets [2]. However, the interaction between Na and Si is so strong that phase transition occurs with the formation of a new stable structure of Na_2Si_2, which can impede the rapid passage of the charge/discharge cycles of such a battery. In contrast, silicene sheets were successfully synthesized on various substrates: Ag, Ir, and ZrB_2 [3–6]. This 2D material is resistant to the intercalation of lithium at room temperature and has extraordinary mechanical and electronic properties. The estimated capacity of the silicene anode can reach about 4200 mA h/g, which characterizes silicene as an excellent new material for an LIB anode.

The quantum-mechanical calculations showed that, without breaking the Si–Si bonds, the capacity of silicene relative to lithium is 1196 mA h/g [7]. Due to the presence of silicene corrugation, the anode made from it has a fair amount of place to accept lithium. The layered structure can play a decisive role in maintaining mechanical integrity in lithium intercalation/deintercalation cycles.

In molecular-dynamic (MD) experiments, lithium adsorption processes were studied in 2D two-layer structures on carbon [8–10] and metal substrates [11–14]. The interaction between silicene and lithium is much stronger than between lithium and graphene [15]. As a result, a silicene sheet can hold more lithium than graphene. According to the DFT estimates [16], the Li/Si ratio in the Li_xSi compound during the adsorption and diffusion of lithium in one- and two-layer silicene can reach up to $x = 1$. Moreover, the number of silicene sheets does not affect the energy of lithium adsorption. The creation of Stone–Wales defects in silicene leads to an increase in the diffusion of lithium through the sheets of this 2D material [17]. The applicability of silicene depends on its ability to bind lithium. How much lithium can be retained and easily removed from the silicene channel on a sub-

strate, while leaving it intact? What effect will the metal substrate have on lithium transport? How will the properties of the 2D structure change, as a result of lithiation and delithiation? These questions still remain open.

The present work is dedicated to a MD study of the possibility of using silicene on an Ni(111) substrate as a new anode material for LIBs. It is also proposed to consider the transport properties of lithium and the effects of size in the sheets of a 2D silicon structure.

Molecular dynamic model. The calculations in the study were performed by the method of classical molecular dynamics. The interatomic interactions in silicene are described by Tersoff's multibody potential [18]. The energy of the pair interaction of i and j atoms taking into account the influence of other atoms (multibody effects) is written as

$$V_{ij} = f_C(r_{ij})\left[A\exp\left(-\lambda^{(1)}r_{ij}\right) - Bb_{ij}\exp\left(-\lambda^{(2)}r_{ij}\right)\right], \quad (1)$$

$$f_C(r_{ij}) = \begin{cases} 1, \\ \frac{1}{2} + \frac{1}{2}\cos\left[\pi\left(r_{ij} - R^{(1)}\right)\Big/\left(R^{(2)} - R^{(1)}\right)\right], \\ 0 \end{cases} \quad (2)$$

$$r_{ij} < R^{(1)}$$
$$R^{(1)} < r_{ij} < R^{(2)},$$
$$r_{ij} > R^{(2)}$$

where r_{ij} is the distance between atoms of i and j, parameters A and B determine the energy characteristics of repulsion and attraction, b_{ij} is the multibody coupling order parameter that describes how the bond energy (attracting part of V_{ij}) is formed with a local atomic arrangement due to the presence of other neighboring atoms. The function f_C decreases from 1 to 0 in the region of $R^{(1)} \le r_{ij} \le R^{(2)}$. Parameters $R^{(1)}$ and $R^{(2)}$ are selected in such a way as to include only the nearest neighbors for consideration. The potential energy is a multiparticle function of the positions of atoms i, j, and k, and is determined by the parameters

$$b_{ij} = \left(1 + \beta^n \xi_{ij}^{n_i}\right)^{-1/(2n)}, \quad (3)$$

$$\xi_{ij} = \sum_{k \ne i,j} f_C(r_{ij}) g(\theta_{ijk}), \quad (4)$$

$$g(\theta_{ijk}) = 1 + \frac{c^2}{d^2} - \frac{c^2}{\left[d^2 + (h - \cos\theta_{ijk})^2\right]}, \quad (5)$$

where parameters n, n_i, and β specify the coupling strength depending on the environment, ξ_{ij} is the effective coordination number that determines the average number of nearest neighbors, taking into account not only the distances between them but also the coupling angle θ_{ijk}. This potential accurately describes the interactions of particles in semiconductors, in which the structure significantly affects the properties of the material. The parameters of this empirical potential are selected from the experiments.

Interactions between Si atoms belonging to different sheets of silicene, as well as Li atoms and ions, were described by the Morse potential [19]

$$\Phi(r) = D_e\left[\exp\{-2\alpha(r - r_e)\} - 2\exp\{-\alpha(r - r_e)\}\right], \quad (6)$$

where D_e is the depth of the potential well, α is the stiffness parameter, and r_e is the equilibrium bond length. The parameters of the Morse potential to describe Si–Si, Li–Li, and Ni–Ni (only considered in order to calculate cross-interactions) interactions have been taken from [19–21]. To represent the Si–Li, Ni–Li, and Si–Ni cross interactions, the parameters are obtained from simple interpolation relations [19]. The interatomic interactions in the nickel substrate have been described using the potential of the embedded atom EAM [22].

The studied system consisted of two sheets of silicene (channel) located on an Ni(111) substrate. The surface of the silicene sheet had a 4 × 4 reconstruction, where 6 of the 18 silicon atoms of a unit cell are displaced by a distance of 0.074 nm perpendicular to the surface up or down for the upper or lower sheets, respectively. According to the earlier MD calculations [23], the optimal values for the channel gap h_g and the distance between the silicene channel and the metal substrate r_{Cu-Si} are 0.75 nm and 0.27 nm, respectively. Perfect silicene sheets contained 300 Si atoms. Monovacancies in these sheets were created by removing silicon atoms in 9 places uniformly distributed over the surface of 2D structure. The initial size $x \times y$ of the silicene sheets of the studied system (before the start of the lithization/delithization cycle) was 4.85 × 4.2 nm. The simulation was performed in the NVT ensemble at 300 K. At the beginning of each calculation (before the implementation of the lithium intercalation process), the system was geometrically optimized during 100 000 time steps.

The intercalation process of lithium consisted of the rhythmic introduction of ions (one-by-one) into the channel, and their subsequent movement, which was directed by a constant electric field of 10^3 V/m. This value of electric field ensures the passage of the lithium ion through the investigated silicene channel, was selected empirically by us in the preliminary MD calculations. When charging modern LIBs with direct current, the electric field in the range of 10^3 to 10^4 V/m is used. There is a proposal for lithium-metal batteries to be charged by pulsed current when the peak field strength reaches 10^6 V/m [24]. The ion that entered the channel and remained in it for 10 ps, acquires an absent electron, and becomes a neutral atom. The filling of the channel with lithium ends as soon as the Li atoms cease to enter the channel. After that, the pro-

Table 1. Characteristics of perfect and defective silicene channel located on an Ni(111) substrate after one cycle of lithization/delithization

Type of vacancy in the silicene sheet	Limit number of lithium atoms intercalated into a channel	Change in channel volume at its maximum filling with lithium and after full deintercalation		Change in the distance between substrate and channel	
		intercalation	deintercalation	intercalation	deintercalation
Perfect	74	−21.8	−5.8%	+30.7%	+64.4%
Monovacancies	91	−10.3%	+2.34%	+59.25%	+51.85%

cess of deintercalation starts. In this case, the field with a strength of 10^5 V/m in the opposite direction removes the Li^+ ion from the channel. The Li atom assigned to exit the channel "loses" the electron, and in the form of an Li^+ ion is removed from the channel under the influence of the electric field. The time allotted for the release of the ion is 20 ps. As a rule, during this time the ion manages to exit the channel.

The LAMMPS code modified by us, which performs parallel computations, was used for the MD calculations [25]. Fragments of the program were introduced to calculate the kinetic and mechanical properties of the system. The calculations were performed on a hybrid cluster-type URAN computer at Institute of Mathematics and Mechanics, Ural Branch, Russian Academy of Sciences, with the peak performance of 216 TFlops/s and a 1864 CPU.

The self-diffusion coefficient of lithium atoms in the silicene channel was calculated through the mean square atomic displacement $\left\langle \left[\Delta \mathbf{r}(t)\right]^2 \right\rangle$

$$D = \lim_{t\to\infty} \frac{1}{2\Gamma t} \left\langle \left[\Delta \mathbf{r}(t)\right]^2 \right\rangle_{t_0}. \quad (7)$$

Here, $\Gamma = 3$ is the dimension of the space. Averaging over the initial moments of time is indicated through $\langle \ldots \rangle_{t_0}$.

The surface roughness of the silicene sheet (or arithmetic mean deviation of the profile) was calculated as in [26],

$$R_a = \frac{1}{N} \sum_{i=1}^{N} |z_i - \overline{z}|, \quad (8)$$

where N is the number of nodes (atoms) on the sheet of silicene, z_i is the displacement of atom i in the direction of axis oz, and $\overline{z}$ is the average value of coordinate z for silicene; z_i and $\overline{z}$ values are determined at the same time.

MD calculation results. The configuration of a silicene channel with monovacancies located on an Ni(111) substrate is shown in Fig. 1. It refers to the moment of completion of one lithization/delithization cycle. The distortions of the sheets indicate that after one lithiation cycle, the shape of the channel is not completely restored to its original state. In addition to information about filling the channel with lithium, Table 1 shows the data on the change in the volume of the silicene channel when the maximum number of lithium atoms is in it and after complete deintercalation. In all cases, except for the completion of lithium deintercalation in the channel from defective silicene, a decrease in the volume of the inter-sheet space is observed. Figure 1 reflects the configuration of the channel with monovacancies, the volume of which increased by 2.34%. After intercalation, the channel with defective walls has a denser filling with lithium (by 23%) than the channel with perfect sheets. This is due to the fact that lithium predominantly occupies free spaces in the 2D structure itself (as confirmed by the ab initio calculations [7]). When the channel is filled, lithium attracts the silicene sheets, and the channel volume decreases. In the case of a silicene channel with the monovacancy defects located on an Ag(111) substrate, identical results were obtained: after completion of intercalation, the channel volume decreased by 3.8%, and after deintercalation it increased by 2.2% [12]. According to the quantum-mechanical calculations, the volume of the silicene channel should not change after a single cycle is performed [16]. During cycling, a significant increase in the distance between the nickel substrate and the adjacent silicene sheet was found in our model (Table 1).

The trajectory of the lithium ion, presented in Fig. 1, shows an example of ion transport inside the channel: from the Li^+_{in} point to the Li^+_{mid} point—the movement of an ion during lithization and the movement of an ion between the Li^+_{in} and Li^+_{mid} points—the delitization process. In addition to the external electric field, which mainly controls the movement of the ion, the field of Si atoms is an important factor. The collision with the atoms of the silicene sheets can significantly correct the trajectory of lithium, bending it and slowing down the transport of ions in the channel.

The image of the horizontal projection of part of the lower sheet of the silicene channel modified by monovacancies and the upper layer of the Ni(111) substrate makes it possible to trace the location of lithium atoms at the time of complete lithization (Fig. 2a). The preferred location of Li is the center of the six-membered Si-ring. Such a location is the energetically most favorable location for the adatom according to the

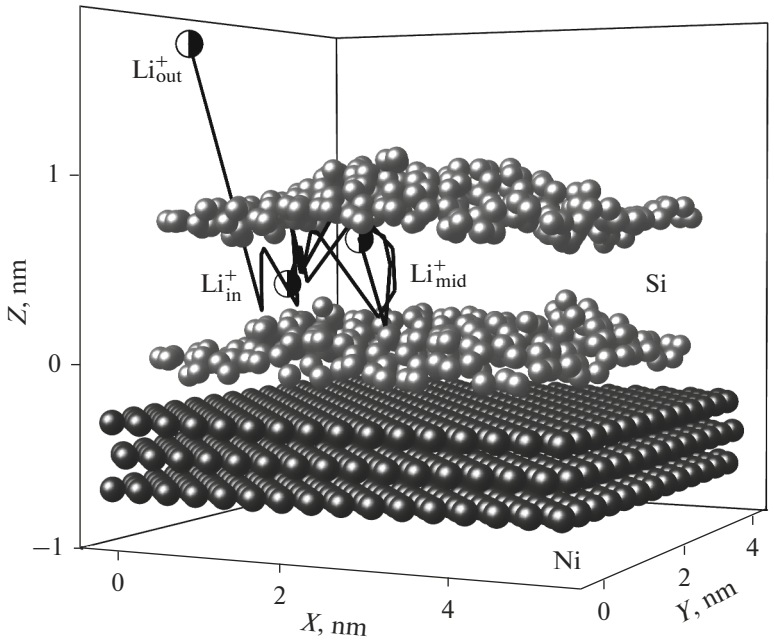

Fig. 1. Configuration of the "two-layer silicene with monovacancies on Ni(111) substrate" system after completion of the full cycle of lithization/delithization; trajectory of one of the lithium ions in the process of lithization (Li^+_{in} and Li^+_{mid} are starting and ending points) and delithization (Li^+_{mid} and Li^+_{out} are starting and ending points).

quantum-mechanical calculations [14, 15]. In the case of lithium adsorption in silicene at concentrations of more than 20% (relative to the number of Si atoms), this location of its atoms is preferable [7] (in comparison with the locations of Li above the middle of the Si–Si bond). The average Li–Si distance obtained in our MD calculations in the case of perfect silicene is 2.55 Å; in the ab initio calculations [7], this value is 2.61 Å. It should be noted that Li introduced into the channel almost never occupies a vacant place in the defect.

In the course of the MD calculation, it was found that not all vacancies retain their original form during the lithization process. Since there was a tendency to reduce the number of dangling bonds that existed at the boundary of the defect, during the calculation, monovacancies were transformed into one 5-membered and one 8-membered rings. Such a rearrangement of the structure is consistent with the ab initio calculations [27].

The horizontal profile of the distribution density of lithium (Fig. 2b) indicates the uneven distribution of the Li atoms along the channel with a small compaction in the middle and more significant compaction at the end of the channel. In the vertical density profile (Fig. 2c), three compaction zones can be distinguished, the most highly populated of which is the zone located closer to the end of the channel. Note that most of the lithium atoms are always located closer to the upper sheet of silicene. Thus, in the case of a channel with defects, 54.9% of the lithium atoms at the time of complete lithization are localized near the top sheet. The fraction of Li atoms in the free space between silicene sheets is small.

During a single cycle, both sheets of the silicene channel turn out to be rather strongly curved (Fig. 3a). Vertical distortion is added to the natural corrugation of silicene (0.074 nm) due to the interaction between the sheets of the 2D structure and lithium, as well as between the sheets and the substrate (distortion is more significant for the lower sheet).

During the filling of the channel with lithium and its deintercalation, the roughness (average vertical deviation) R_a of both the upper and lower sheets of silicene changes nonmonotonically (Fig. 3b). The vertical middle line in the form of a dashed line (shown in Figs. 4, 5) corresponds to the maximum degree of channel saturation with lithium. This line passes through the value of $N_{Li} = 91$ (number of lithium atoms in the channel), when monovacancies are present in the silicene sheets. Both in lithization and delithization, the R_a value at the end of the process is higher than at its beginning. At the same time, the R_a of the lower sheet is almost always lower than that of the upper one, which indicates the stabilizing effect of the nickel substrate. In addition, more lithium atoms are attached to the top sheet of silicene than to the lower one. This creates an additional degree of roughness. On the average, after a single cycle, the roughness of the silicene channel obtained in these MD cal-

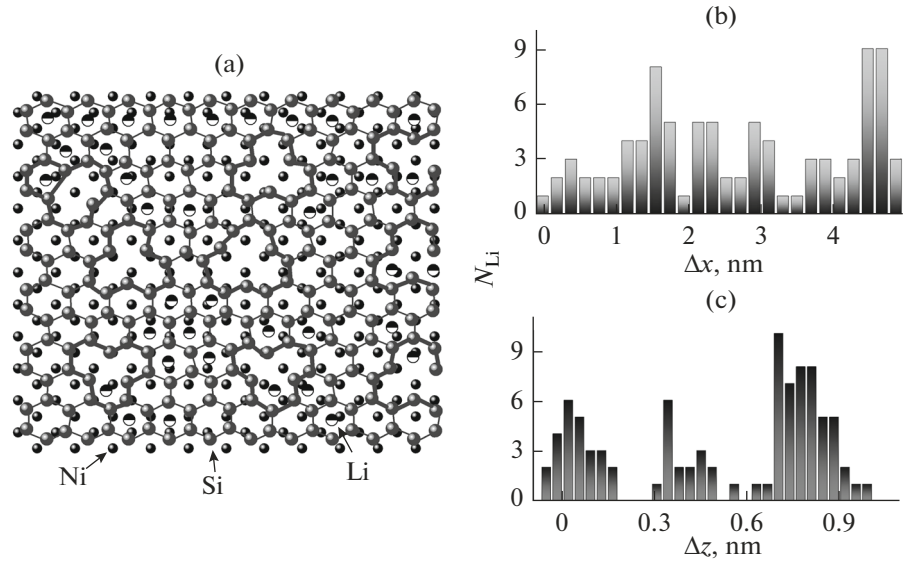

Fig. 2. Schematic representation of the horizontal projection of a portion of the lower silicene sheet with monovacancies on the Ni(111) substrate layer and distribution of lithium over the sheet surface (a); horizontal (longitudinal) (b) and vertical (c) lithium density profiles in a silicene channel with monovacancies on Ni(111) substrate.

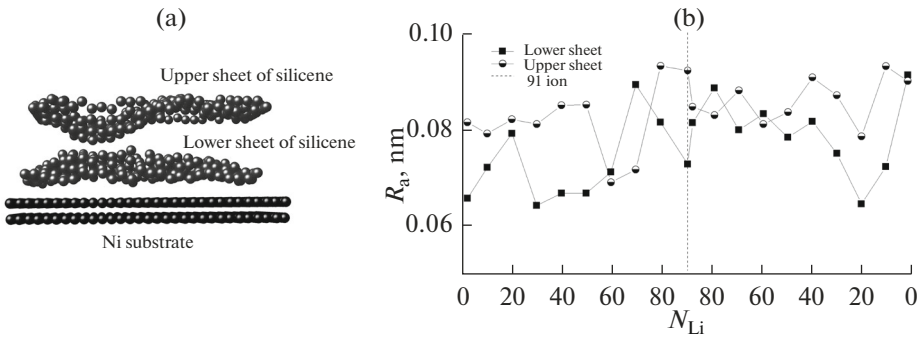

Fig. 3. Schematic representation (*xz*-projection) of the arrangement of silicene channel on an Ni(111) substrate after completion of the intercalation/deintercalation cycle of Li (a); change in the roughness of the lower and upper sheets of silicene with monovacancies on an Ni(111) substrate during intercalation (left of the dashed line) and deintercalation (on right) of lithium (b).

culations on an Ni(111) substrate is lower than in the similar MD studies on Ag(111) or Cu(111) substrates [11–14].

The specific internal energy U_{Li} of Li atoms decreases with an increase in their number during intercalation. One of the factors leading to this result is related to the ionic pushing of Li atoms to energetically more favorable positions (Fig. 4). A particularly strong effect of the Li^+ ion on its related atoms, which causes a decrease in U_{Li}, is observed at the initial stage of intercalation, when the channel contains no more than 20 Li atoms. At the beginning of deintercalation, the energy of U_{Li} may decrease due to the ongoing structural relaxation. Then it takes approximately constant values, and at the very end of deintercalation increases significantly, because the fraction of kinetic energy in this period becomes dominant. The insets on the right show fragments of the configurations of perfect silicene and silicene modified with monovacancies during deintercalation, when $N_{Li} = 25$. On the average, the internal energy of the lithium atoms introduced in the channel made of perfect silicene (–1.5 eV/atom) is 7.5% lower than the energy of lithium atoms intercalated into a channel with sheets containing monovacancies (–1.42 eV/atom).

Figure 5a shows the displacement of a lithium atom along the surface of a defective silicene sheet after intercalation into the channel. When the channel is filled with a small number of lithium atoms, a newly appearing electrically neutral Li atom, without experiencing the action of the external field, moves rectilinear translational until it is fixed above the center of the six-membered ring (the most advantageous position of the adatom in the plane of a 2D structure [7]). Subse-

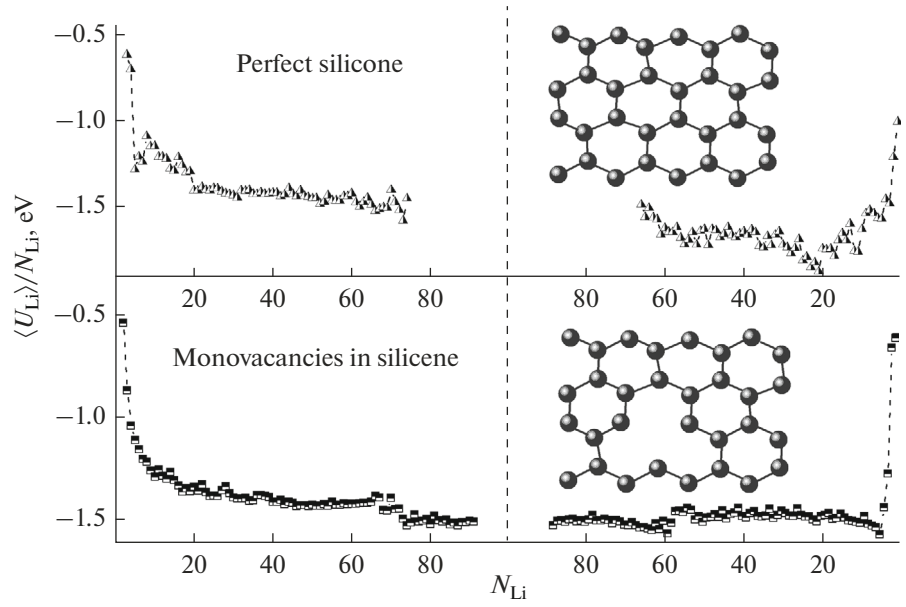

Fig. 4. Internal energy of lithium atoms during intercalation (left) and deintercalation (right) in the perfect and defective silicene channels on the Ni(111) substrate, N_{Li} is the number of lithium atoms in the channel; the insets in the right show planar configurations of perfect silicene and silicene modified with monovacancies when 25 Li atoms are in the channel.

quently, as the channel is filled with lithium, the atom performs only oscillatory motions near this equilibrium point in the channel.

The self-diffusion coefficient D of Li atoms exhibits strong fluctuations at the initial stage of intercalation, which is related to the sufficiently large freedom to move the Li^+ ion in a poorly filled channel (Fig. 5b). Then the values of coefficient D either stabilize for a short period (as is the case with perfect silicene sheets), or immediately increase (the case of sheets with monovacancies) due to the intense structural rearrangement of the packing of Li atoms. The behavior of the D value at the initial stage of deintercalation strongly depends on the presence or absence of defects in silicene. At the final stage of deintercalation, coefficient D, as a rule, increases, because the movement of the ion in the channel becomes increasingly freer. The average value of D_{Li} for a system with perfect silicene sheets is 3.67×10^{-5} cm^2/s, and for a channel with defective silicene walls, it is 1.48×10^{-5} cm^2/s. The large occupancy of the channel by lithium in the case of monovacancies in the sheets prevents the intensive movement of Li atoms, causing a decrease in the self-diffusion coefficient. For comparison, the experimental value of the diffusion coefficient of lithium in a similar 2D structure, bilayer graphene, is estimated to be 7×10^{-5} cm^2/s [28].

CONCLUSIONS

In a MD experiment, the process of intercalation/deintercalation of lithium (cycling) in the two-layer silicene on an Ni(111) substrate system has been considered. It is shown that a perfect silicene channel can contain up to 74 lithium atoms, and a channel modified by monovacancies can contain up to 91 lithium atoms. In this case, the Si–Si bonds of the 2D structure are not destroyed. During the entire single cycle (up to 2.5 ns), similar systems of the same type, having defects in silicene in the form of mono-, bi-, and trivacancies, are stable; however, in the presence of hexavacancies, the tendency to the destruction of silicene is present in them. The most energetically advantageous arrangement of intercalated lithium in the channel is its location above the centers of six-membered silicon rings. Moreover, the upper silicene sheet is 15–20% more filled with lithium than the lower one. The interaction between lithium and silicene is quite strong. Having found its energetically most favorable position, the lithium atom oscillates around it, and does not move along the channel. No tendencies toward the formation of lithium clusters (which may become the initial phase of dendrite nucleation) were observed in the model. This indicates the stability of the silicene anode relative to working cycles executing. At the same time, the interaction of lithium with a 2D structure is not sufficiently strong to lead to the destruction of the silicene lattice. The self-diffusion coefficient of lithium atoms as a whole is an increasing (during intercalation) and decreasing (during deintercalation) function of the number of Li atoms in a perfect channel. Values of D_{Li} monotonically fluctuate when silicene sheets contain monovacancies. On the average, the D_{Li} value for a system with

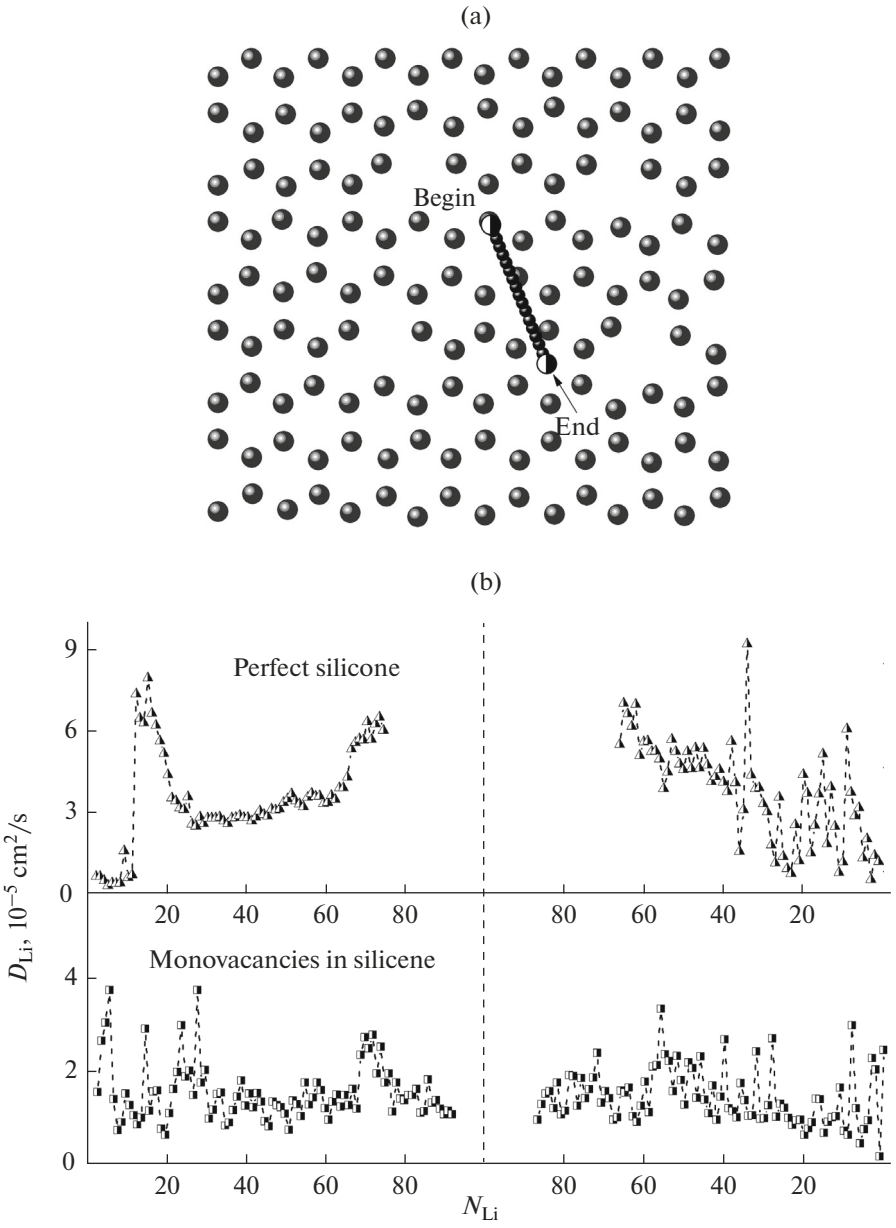

Fig. 5. Schematic representation of the displacement of a lithium atom along the surface of a defective silicene sheet (a); self-diffusion coefficient of lithium during intercalation (left) and deintercalation (right) in perfect and defective (with monovacancies) silicene channels on an Ni(111) substrate (b).

perfect silicene sheets is noticeably higher than for a channel with defective walls.

The Ni(111) substrate proves to be a reliable material for supporting a two-layer silicene channel. Unlike other metals (Ag, Cu), the channel does not change its volume at the end of one intercalation/deintercalation cycle and has generally moderate roughness values.

The widespread prevalence of silicon, high capacity of silicene towards lithium adsorption, flexibility of the 2D structure, and the small barrier for the diffusion of lithium in the channel can ensure the priority use of silicene in LIBs. The use of a nickel substrate in a silicene anode will make it possible to obtain high energy density and extend the LIB life cycle.

FUNDING

This work is performed in the framework of the Agreement no. 075-03-2020-582/1, dated February 18, 2020 (topic no. 0836-2020-0037).

CONFLICT OF INTEREST

The authors declare that they have no conflict of interest.

REFERENCES

1. Huang, T., Tian, B., Guo, J., Shu, H., Wang, Y., and Dai, J., Semiconducting borophene as a promising anode material for Li-ion and Na-ion batteries, *Mater. Sci. Semicond. Process.,* 2019, vol. 89, pp. 250–255.
2. Xu, S., Fan, X., Liu, J., Jiang, Q., Zheng, W., and Singh, D.J., Adsorption of Na on silicene for potential anode for Na-ion batteries, *Electrochim. Acta,* 2019, vol. 297, pp. 497–503.
3. Chiappe, D., Scalise, E., Cinquanta, E., Grazianetti, C., Broek, B., Fanciulli, M., Houssa, M., and Molle, A., Two-dimensional Si nanosheets with local hexagonal structure on a MoS_2 surface, *Adv. Mater.,* 2014, vol. 26, no. 13, pp. 2096–2101.
4. Fleurence, A., Friedlein, R., Ozaki, T., Kawai, H., Wang, Y., and Yamada-Takamura, Y., Experimental evidence for epitaxial silicene on diboride thin films, *Phys. Rev. Lett.,* 2012, vol. 108, no. 24, 245501.
5. Tao, L., Cinquanta, E., Chiappe, D., Grazianetti, C., Fanciulli, M., Dubey, M., Molle, A., and Akinwande, D., Silicene field-effect transistors operating at room temperature, *Nat. Nanotechnol.,* 2015, vol. 10, no. 3, pp. 227–231.
6. Wang, M., Liu, L., Liu, C.-C., and Yao, Y., Van der Waals heterostructures of germanene, stanine, and silicene with hexagonal boron nitride and their topological domain walls, *Phys. Rev. B,* 2016, vol. 93, no. 15, 155412.
7. Xu, S., Fan, X., Liu, J., Singh, D.J., Jiang, Q., and Zheng, W., Adsorption of Li on single-layer silicene for anodes of Li-ion batteries, *Phys. Chem. Chem. Phys.,* 2018, vol. 20, no. 12, pp. 8887–8896.
8. Galashev, A.Y. and Zaikov, Yu.P., *Properties and Application of Ultrathin Carbon and Silicon Films,* New York: Nova Science, 2018.
9. Galashev, A.Y. and Ivanichkina, K.A., Computer study of the properties of silicon thin films on graphite, *Russ. J. Phys. Chem A,* 2017, vol. 91, no. 12, pp. 2448–2452.
10. Galashev, A.Y., Rakhmanova, O.R., and Ivanichkina, K.A., Graphene and graphite supports for silicene stabilization: A computer study, *J. Struct. Chem.,* 2018, vol. 59, no. 4, pp. 877–883.
11. Galashev, A.Y., Ivanichkina, K.A., Vorob'ev, A.S., and Rakhmanova, O.R., Structure and stability of defective silicene on Ag(001) and Ag(111): A computer experiment, *Phys. Solid State,* 2017, vol. 59, no. 6, pp. 1242–1252.
12. Galashev, A.Y. and Ivanichkina, K.A., Computer study of atomic mechanisms of intercalation/deintercalation of Li ions in a silicene anode on an Ag(111) substrate, *J. Electrochem. Soc.,* 2018, vol. 165, pp. A1788–A1796.
13. Galashev, A.Y., Ivanichkina, K.A., Rakhmanova, O.R., and Zaikov, Yu.P., Physical aspects of the lithium ion interaction with the imperfect silicene located on a silver substrate, *Lett. Mater.,* 2018, vol. 8, no. 4, pp. 463–467.
14. Galashev, A.Y. and Ivanichkina, K.A., Computer test of a new silicene anode for lithium-ion batteries, *Chem. Electrochem.,* 2019, vol. 6, no. 5, pp. 1525–1535.
15. Lin, X.Q. and Ni, J., Much stronger binding of metal adatoms to silicene than to graphene: A first-principles study, *Phys. Rev. B: Condens. Matter Mater. Phys.,* 2012, vol. 86, no. 7), 075440.
16. Tritsaris, G.A., Kaxiras, E., Meng, S., and Wang, E., Adsorption and diffusion of lithium on layered silicon for Li-ion storage, *Nano Lett.,* 2013, vol. 13, no. 5, pp. 2258–2263.
17. Xin, Y. and Yu, Y.-X., Adsorption and mobility of lithium on pristine and Stone–Thrower–Wales defective silicene, in *Proceedings of the International Conference on Materials Chemistry and Environment Protection MEEP 2015,* Amsterdam: Atlantis, 2015, pp. 50–54.
18. Tersoff, J., Chemical order in amorphous silicon carbide, *Phys. Rev. B: Condens. Matter Mater. Phys.,* 1994, vol. 49, no. 23, pp. 16349–16352.
19. Yu, R., Zhai, P., Li, G., and Liu, L., Molecular dynamics simulation of the mechanical properties of single-crystal bulk Mg_2Si, *J. Electron. Mater.,* 2012, vol. 41, pp. 1465–1469.
20. Das, S.K., Roy, D., and Sengupta, S., Volume change in some substitutional alloys using Morse potential function, *J. Phys. F: Met. Phys.,* 1977, vol. 7, no. 1, pp. 5–14.
21. Li, M. and Wang, Y., Molecular-dynamics simulation of the Ag/Ni interface, *Appl. Phys. A,* 1995, vol. 61, no. 4, pp. 431–434.
22. Foiles, S.M., Baskes, M.I., and Daw, M.S., Embedded-atom-method functions for the fcc metals Cu, Ag, Au, Ni, Pd, Pt, and their alloys, *Phys. Rev. B: Condens. Matter Mater. Phys.,* 1986, vol. 33, no. 12, pp. 7983–7991.
23. Rakhmanova, O.R. and Galashev, A.Y., Motion of a lithium ion over a graphene-silicene channel: A computer model, *Russ. J. Phys. Chem. A,* 2017, vol. 91, no. 5, pp. 921–925.
24. Li, Q., Tan, S., Li, L., Lu, Y., and He, Y., Understanding the molecular mechanism of pulse current charging for stable lithium-metal batteries, *Sci. Adv.,* 2017, vol. 3, no. 7, e1701246.
25. Plimpton, S.J., Fast parallel algorithms for short-range molecular dynamics, *J. Comput. Phys.,* 1995, vol. 117, no. 1, pp. 1–19.
26. Galashev, A.E. and Polukhin, V.A., Removal of copper from graphene by bombardment with argon clusters: Computer experiment, *Phys. Met. Metallogr.,* 2014, vol. 115, no. 7, pp. 697–704.
27. Berdiyorov, G.R. and Peeters, F.M., Influence of vacancy defects on the thermal stability of silicene: A reactive molecular dynamics study, *RSC Adv.,* 2014, vol. 4, no. 3, pp. 1133–1137.
28. Kuhne, M., Paolucci, F., Popovich, J., and Ostrovsky, P., Ultrafast lithium diffusion in bilayer graphene, *Nat. Nanotechnol.,* 2017, vol. 12, no. 9, pp. 895–901.

Translated by Sh. Galylatdinov